Transmission Line Model for an Edge-Coupled Patch Antenna

Wiset Saksiri, Mitchai Chongcheawchamnan, and Monai Krairiksh

In this paper, a simple transmission line model for an edge-coupled patch antenna is presented. The coupled section is modeled with a lump network which represents the mutual admittance between patches and from patch to ground. Theoretical analysis of two edge-coupled patch antenna models are compared by simulation and experiment in antennas designed to operate at the 2 GHz band. The proposed model predicts the return loss of the antenna accurately.

Keywords: Serrate coupling, edge-coupled patch antenna, bandwidth, transmission line model.

I. Introduction

As broadband wireless communications are becoming more important in daily life, each subsystem in a wireless transceiver supporting such applications must be able to support enough information bandwidth [1]. Fundamentally, this is achieved simply with wideband design.

Wideband antenna is one of the key subsystems for achieving a broadband wireless transceiver. In the past, the patch antenna gained a great deal of interest due to its low profile and light weight [2]. Basically a patch and a ground forming a patch antenna create a microwave cavity which can resonate at many frequencies. However, the patch usually operates around one resonance frequency of narrow bandwidth. Numerous studies have proposed ways to enhance patch antenna bandwidth and reduce antenna size by, for example, composing an impedance matching network with the antenna's structure through stacked geometry [3], employing coplanar geometry with a tuning stub [4], forming additional resonators with slots [5], designing an antenna with a thick substrate [6], and applying edge-coupled antenna topology (parallel [7] or serrate coupling [8]). Among these, edge-coupled patch antennas employing parallel and serrate coupling are of interest to us because of their compact design, wideband operation, and simple integration.

For the first time, this paper presents an edge-coupled patch antenna with a simple transmission line model. Developing this model will facilitate the design process. The transmission line model proposed is based on the transmission line model for a shorted patch antenna. Section II details the complete transmission line model of the coupled patch antenna. In section III, we compare the results from the theoretical analysis based on the transmission line model are with the electromagnetic (EM) simulation results and the measured results. Finally, the paper

Manuscript received Apr. 3, 2008; revised June 18, 2008; accepted June 27, 2008.

This work was supported by the Thailand Research Fund under the Grant number RTA-4880002.

Wiset Saksiri (phone: + 6629883666 ext. 149, email: wiset@kmutnb.ac.th) is with the Department of Electrical Engineering, Mahanakorn University of Technology, Bangkok, Thailand.

Mitchai Chongcheawchamnan (phone: + 66074287404, email: mitchai@ieee.org) is with the Department of Computer Engineering, Faculty of Engineering, Prince of Songkla University, Hat Yai, Songkla, Thailand.

Monai Krairiksh (email: kkmonai@kmitl.ac.th) is with the Department of Telecommunication Engineering, King Mongkut's Institute of Technology Ladkrabang (KMITL), Bangkok, Thailand.

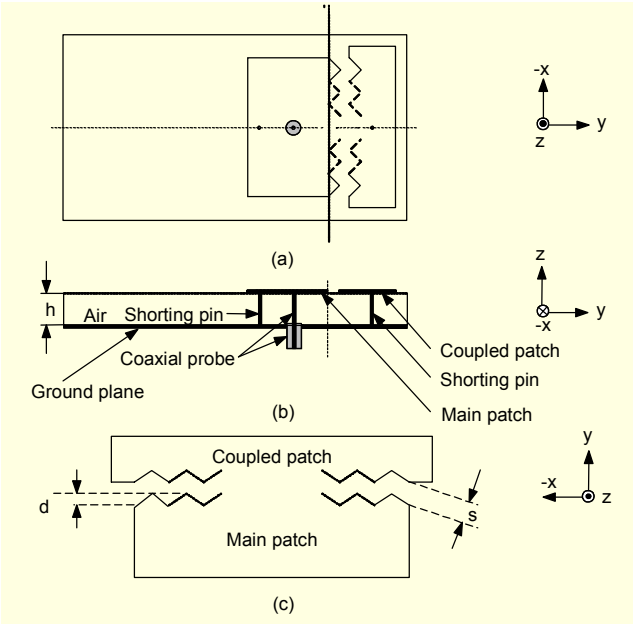

Fig. 1. Serrate-coupled patch antenna.

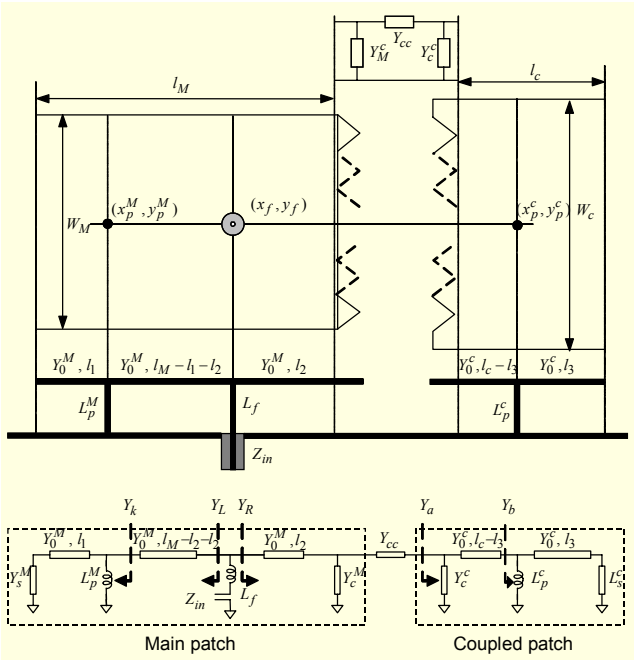

Fig. 2. Transmission line model of a coupled patch antenna.

concludes in section IV.

II. Transmission Line Model

Currently, there are two edge-coupled patch antenna topologies: parallel-coupled or serrate-coupled. We use the structure of a serrate-coupled patch antenna as an example since this structure is more common than that of a parallel-coupled patch. Typically, an edge-coupled patch antenna comprises a main patch and a coupled patch. The two patches are separated by a gap of distance *s*. There are two shorting pins located between the main and coupled patches which are laminated on the substrate of thickness *h*. The shorting pins and a feed probe are located in the middle of the patches. As in the short patch antenna design [9], the use of a shorting pin with each patch makes it possible to miniaturize the patch size, and a signal is applied through a feed coaxial probe at the main patch. Fundamentally, an edge-coupled patch antenna has two frequency resonances controlled by the patch dimensions, shorting pins, and feed parameters.

Mutual coupling between two patches draws or separates these two resonances, and this, in turn, modifies the antenna impedance bandwidth. Choosing the serrate-coupled section provides more degrees of freedom in adjusting the impedance bandwidth of the antenna [8]. In Fig. 1(c), all serrate elements have uniform shapes. The serrate depth and number are denoted by *d* and *N*, respectively.

1. Antenna Model and Input Impedance

To calculate the input impedance characteristic of an edge-coupled patch antenna, the transmission line model shown in Fig. 2 is proposed. The patch of width *W*, which is already known, can be effectively modeled with a transmission line of characteristic admittance Y_0. Let γ_i and Y_0^i denote the propagation constant and characteristic admittance of patch *i*, where *i* is either *M* or *C*, representing the main or coupled patch, and Y_s^i denotes the admittances associated with the radiation slot of the patch. By inspection, the input impedance (Z_{in}) in Fig. 2 can be written as

$$Z_{in} = j\omega L_f + (Y_L + Y_R)^{-1}, \tag{1}$$

where Y_L and Y_R are the driving-point admittances defined in Fig. 2. We can determine Y_L from

$$Y_L = Y_0^M \left[\frac{Y_k + Y_0^M \tanh \gamma_M (l_M - l_1 - l_2)}{Y_0^M + Y_k \tanh \gamma_M (l_M - l_1 - l_2)} \right], \tag{2}$$

where

$$Y_k = \frac{1}{j\omega L_p^M} + Y_0^M \frac{Y_s^M + Y_0^M \tanh \gamma_M l_1}{Y_0^M + Y_s^M \tanh \gamma_M l_1}. \tag{3}$$

For Y_R shown in Fig. 2, we obtain

$$Y_R = Y_0^M \left[\frac{Y_c^M + (1/Y_{CC} + 1/Y_a)^{-1} + Y_0^M \tanh \gamma_M l_2}{Y_0^M + \left\{ Y_c^M + (1/Y_{CC} + 1/Y_a)^{-1} \right\} \tanh \gamma_M l_2} \right], \tag{4}$$

where Y_a is given by

$$Y_a = Y_C^C + Y_0^C \frac{Y_b + Y_0^C \tanh\gamma_C\left(l_C - l_3\right)}{Y_0^C + Y_b \tanh\gamma_C\left(l_C - l_3\right)}, \quad (5)$$

and

$$Y_b = \frac{1}{j\omega L_p^C} + Y_0^C \frac{Y_s^C + Y_0^C \tanh\gamma_C l_3}{Y_0^C + Y_s^C \tanh\gamma_C l_3}. \quad (6)$$

Note that the inductance of the feed probe or shorting pin in (1), (3), and (6) can be calculated by [10]

$$L = \frac{\eta_0 h}{2\pi c}\ln\left[\frac{4c}{\zeta\omega d\sqrt{\varepsilon_r}}\right], \quad (7)$$

where $\zeta = 1.781072$, h is the length of the feed or the shorting pin, d is the diameter, η_0 is the intrinsic impedance of free space, and c is the light velocity.

2. Determining Y_0^i and Y_s^i

The slot admittance Y_s^i is composed of the conductance and susceptance, which are related to the power radiated from the slot and the stored energy:

$$Y_s^i = G_s^i + jB_s^i. \quad (8)$$

The conductance of the radiating slot (either main or coupled patch) at the operating wavelength is applied [11] to determine the self conductance G_s^i, which may be calculated as

$$G_s^i = \frac{1}{\omega\eta_0}\left\{\left(\omega Si(\omega) + \frac{\sin\omega}{\omega} + \cos\omega - 2\right)\left(1 - \frac{k_0^2\Delta l_i^2}{24}\right) + \frac{k_0^2\Delta l_i^2}{12}\left(\frac{1}{3} + \frac{\cos\omega}{\omega^2} - \frac{\sin\omega}{\omega^3}\right)\right\}, \quad (9)$$

where k_0 is the free-space wave number, Δl_i is the excess length, and $Si(\omega)$ is the sine integral function. The radiating slot suseptance (B_s^i) is given by

$$B_s^i = Y_0^i \tan\left(\beta_i \Delta l_i\right). \quad (10)$$

Kirschning proposed an expression for the excess length Δl_i derived from field-theoretical data applying a curve fitting procedure:

$$\Delta l_i = h\frac{\xi_1 \cdot \xi_3 \cdot \xi_5}{\xi_4}, \quad (11),$$

where ξ_1, ξ_3, ξ_4, and ξ_5 are defined in [12].

Normally, the patch width is larger than the substrate thickness, that is, $W/h \geq 1$. The characteristic admittances of the main and coupled patches can be computed by

$$Y_0^i = \left[Z_0^i\left(\varepsilon_r, f = 0\right)\cdot\left(\frac{R_{13}}{R_{14}}\right)^{R_{17}}\right]^{-1}, \quad (12)$$

where R_{13}, R_{14}, and R_{17} are given as in [13]. The characteristic impedance of the line at zero frequency is given by

$$Z_0^i\left(\varepsilon_r, f = 0\right) = \frac{Z_0\left(\varepsilon_r = 1\right)}{\sqrt{\varepsilon_{eff}\left(f = 0\right)}}, \quad (13)$$

where the effective dielectric constant at zero frequency (13) can be found easily in various textbooks.

Accurate equations for calculating characteristic impedance can be commonly found. However, for an air substrate, Hammerstad proposed the following revised formulas for high accuracy characteristic impedance:

$$Z_0^i\left(\varepsilon_r = 1\right) = 60\ln\left[\frac{F_1}{W_i/h} + \sqrt{1 + \left(\frac{2}{W_i/h}\right)^2}\right], \quad (14)$$

where

$$F_1 = 6 + \left(2\pi - 6\right)\exp\left[-\left(30.666\frac{h}{W_i}\right)^{0.7528}\right]. \quad (15)$$

3. Model for Coupled Section

A model for a coupled section in either parallel or serrate form is presented in Fig. 3. The model consists of two shunt admittances (Y_C^M, Y_C^C), representing the distributed fields beneath main and coupled patches, and a series admittance (Y_{CC}), describing the field coupling between the patches. These parameters are related to the following two-port Y-parameters:

$$Y_{CC} = -Y_{12}, \quad (16)$$

$$Y_C^C = Y_{22} + Y_{12}, \quad (17)$$

$$Y_C^M = Y_{11} + Y_{12}. \quad (18)$$

The Y parameters (Y_{11}, Y_{12}, Y_{21}, Y_{22}) can be calculated from the S-parameters as follows:

$$Y_{11} = Y_0\frac{(1 - S_{11})(1 + S_{22}) + S_{12}S_{21}}{(1 + S_{11})(1 + S_{22}) - S_{12}S_{21}}, \quad (19)$$

$$Y_{12} = Y_0\frac{-2S_{12}}{(1 + S_{11})(1 + S_{22}) - S_{12}S_{21}}, \quad (20)$$

$$Y_{21} = Y_0\frac{-2S_{21}}{(1 + S_{11})(1 + S_{22}) - S_{12}S_{21}}, \quad (21)$$

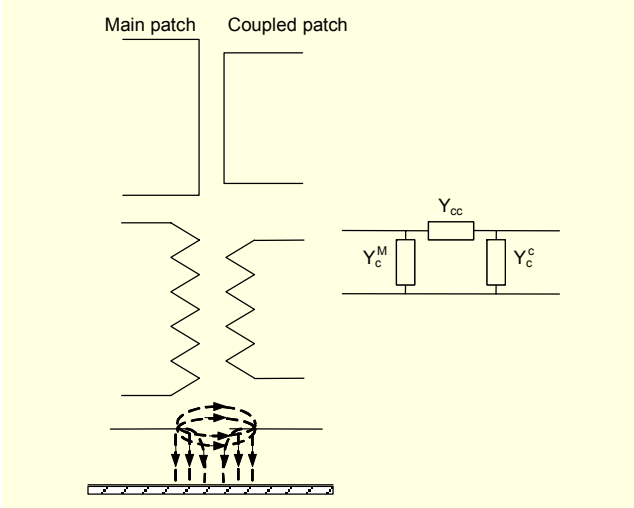

Fig. 3. Circuit model for a coupled section.

$$Y_{22} = Y_0 \frac{(1+S_{11})(1-S_{22})+S_{12}S_{21}}{(1+S_{11})(1+S_{22})-S_{12}S_{21}}, \qquad (22)$$

where Y_0 is the normalized admittance. Since there is no accurate closed form equation for characterizing the coupled section, we resort to the simulated results to evaluate the model elements of the coupled section.

III. Results and Discussion

Validation of our analysis is demonstrated and discussed in this section. Two edge-coupled antennas, one with parallel-coupled patches and the other with serrate-coupled patches, are our study examples. The parallel-coupled design presented in [7] was selected, whereas the serrate-coupled patch antenna was newly designed. The measured return losses of these antennas are compared with the EM simulated and computed results obtained using IE3D software. The radiation pattern and gain of the serrate-coupled design are also reported. It should be noted that all EM simulated results obtained are for infinite ground plane antennas.

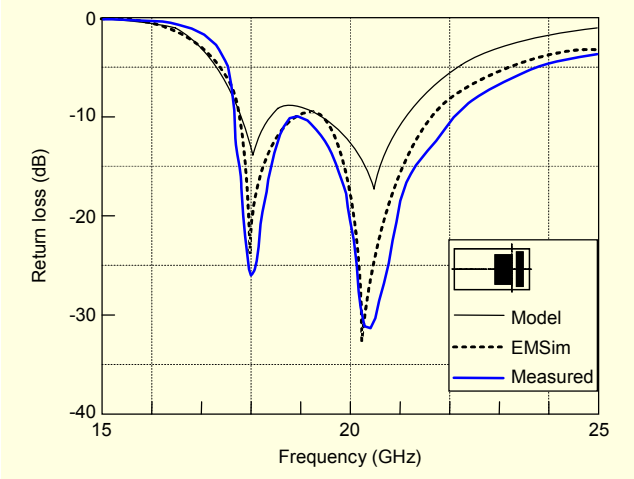

Fig. 4. Return loss results of the parallel-coupled patch antenna.

1. Parallel-Coupled Design

Table 1 shows the antenna parameters given in [7]. Figure 4 compares the return loss results predicted for the proposed model with the EM simulated and measured results. The transmission line model predicts two resonant frequencies at 1.8 GHz and 2.05 GHz, which are rather close to the resonant frequencies obtained from the EM simulation and measurement.

2. Serrate-Coupled Design

Figure 5 shows a photograph of the serrate-coupled patch antenna whose parameters are summarized in Table 1. Note that the ground plane size is intentionally large for good radiation performance.

The size of the antenna, including the ground plane, is around 4.5 cm × 9 cm. Figure 6 shows the return loss result predicted from the model compared with the EM and measured results**.** The transmission line model can predict two resonant frequencies that are rather close to those of the measured results. The difference in magnitude response obtained from the model and measurement may be due to the radiation of the side slot being neglected and mutual interaction

Table 1. Parameters of coupled patch antennas.

Parameter	Parallel (mm)	Serrate (mm)
W_M	30	30
W_C	33	33
L_M	20	20
L_C	10	10
s	8	8
N	-	7
d	-	3
h	10	10
ε_r	1	1
r_f	0.3125	0.3215
r_p	0.3125	0.3125
t	0.1	0.1
(x_p^M, y_p^M)	(0, -13.5)	(0, -13.5)
(x_p^C, y_p^C)	(0, 14.5)	(0, 14.5)
(x_f, y_f)	(0, -5,6)	(0, -5,6)

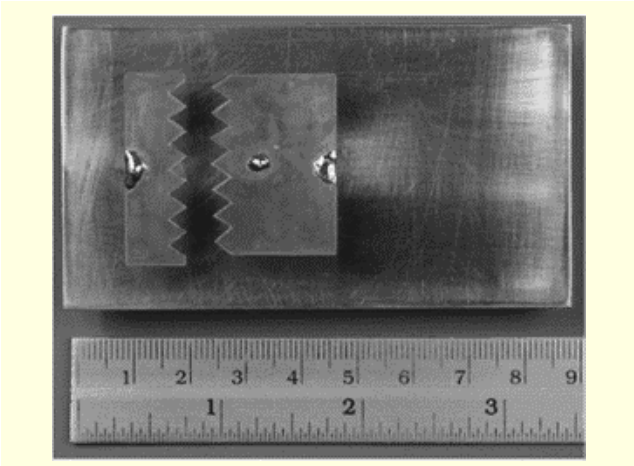

Fig. 5. Photograph of the serrate-coupled patch antenna.

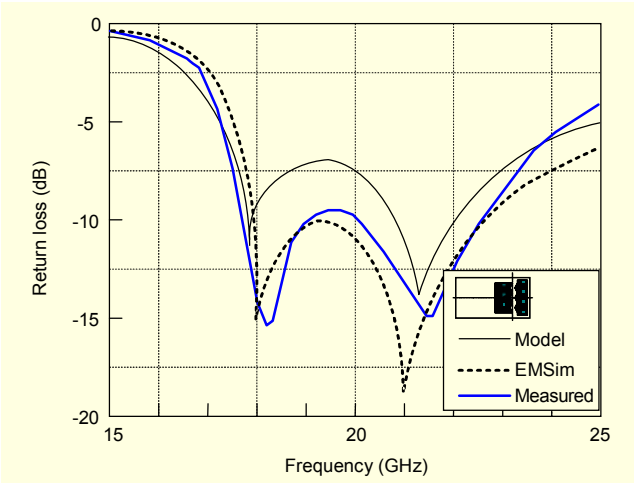

Fig. 6. Return loss of the proposed serrate-coupled antenna.

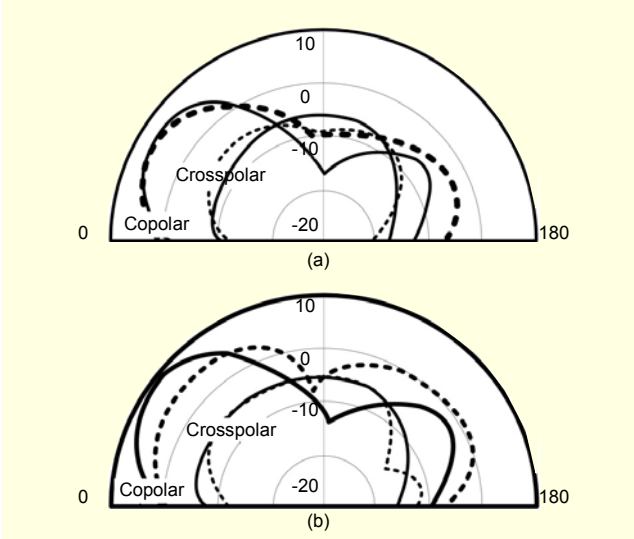

Fig. 7. Computed (solid line) and measured (dotted line) radiation patterns: (a) 1.78 GHz and (b) 2.15 GHz.

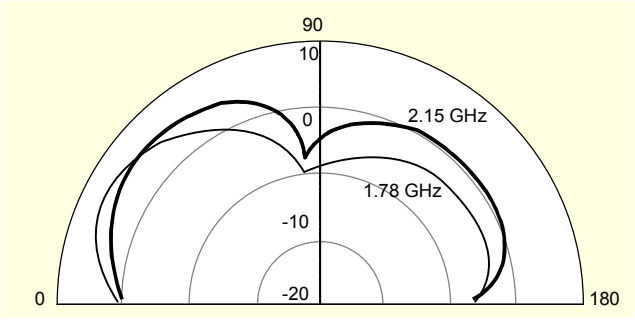

Fig. 8. Measured antenna gain.

between slots in the same patch and different patches.

Figure 7 shows the simulated and measured radiation patterns at 1.78 GHz and 2.15 GHz. The measured antenna gains at 1.78 GHz and 2.15 GHz are 7.5 dBi and 7 dBi, respectively, as shown in Fig. 8.

IV. Conclusion

For the first time, a transmission-line model for an edge-coupled patch antenna has been demonstrated. The patches function as frequency resonators which are coupled with a mutual admittance. With this coupling mechanism, the bandwidth of the edge-coupled patch antenna can be larger than that of a single shorted patch antenna if an appropriate coupling is chosen. A serrate-coupled patch antenna is one solution which has a greater degree of freedom to achieve a wide bandwidth antenna. The accuracy of the model can be further enhanced if mutual interaction of slots in the same patch and different patches is included.

Acknowledgments

The authors are very grateful to valuable suggestions from anonymous reviewers.

References

[1] T.S. Rappaport, *Wireless Communications: Principles and Practice*, 2nd ed., Upper Saddle River, New Jersey, Prentice-Hall, Inc., 2002.

[2] D.M. Pozar, "Microstrip Antenna," *Proc. IEEE*, vol. 80, no. 1, Jan. 1992, pp. 79-81.

[3] B.L. Ooi, S. Qin, and M.S. Leong, "Novel Design of Broad-Band Stacked Patch Antenna," *IEEE Trans. Antennas Propagat*, vol. 50, no. 10, Oct. 2002, pp. 1391-1395.

[4] H.D. Chen, "Broadband CPW-Fed Square Slot Antennas with a Widened Tuning Stub," *IEEE Trans. Antennas Propagat.*, vol. 51, no. 8, Aug. 2003, pp. 1982-1986.

[5] J.H. Lu, "Broadband Dual-frequency Operation of Circular Patch Antenna and Arrays with a Pair of L-Shaped Slots," *IEEE Trans. Antennas Propagat.*, vol. 51, no. 5, May 2003, pp. 1081-1023.

[6] N. Herscovici, "A Wideband Single Layer Patch Antenna," *IEEE Trans. Antennas Propagat.*, vol. 46, no. 4, Apr. 1998, pp. 471-474.

[7] Y.J. Wang, C.K. Lee, and W.J. Koh, "Design of Small and Broad-Band Internal Antennas for IMT-2000 Mobile Handsets," *IEEE Trans. Microwave Theory and Tech.*, vol. 49, no. 8, Aug. 2001, pp. 1398-1403.

[8] W. Saksiri and M. Krairiksh, "A Couple Microstrip Antenna Employing Serrated Coupling," *IEEE Microwave and Wireless Component Lett.*, vol. 15, Feb. 2005, pp. 77-79.

[9] Y.X. Gao, K.M. Luk, and K.F. Lee, "Dual-band Slot-Loaded Short-Circuited Patch Antenna," *IEEE Antenna and Propagation Society International*, vol. 3, July 2000, pp. 1592-1595.

[10] R.W. Dearnley and A.F. Barel, "A Broad-Band Transmission Line Model for a Rectangular Microstrip Antenna," *IEEE Trans. Antenna and Propagation*, vol. 37, no. 1, Jan. 1989, pp. 6-15.

[11] H. Pues and A. Van de Capelle, "Accurate Transmission-Line Model for the Rectangular Microstrip Antenna," *Proc. IEE*, vol. 131, no. 6, Dec. 1984, pp. 334-340.

[12] M. Kirschning, R.H. Jansen, and N.H.L. Koster, "Accurate Model for Open End Effect of Microstrip Lines," *Electron. Lett.*, vol. 17, 1981, pp. 123-125.

[13] G. Kompa, *Practical Microstrip Design and Applications*, Artech House, 2005.

Wiset Saksiri received the BS and MS degrees in electrical engineering from King Mongkut's Institute of Technology, Bangkok, Thailand, in 1995 and 2000, respectively. He is currently working toward a DEng degree in electrical engineering at Mahanakorn University of Technology, Bangkok, Thailand. He is a lecturer with the Department of Technical Training in Electrical Engineering, Faculty of Technical Education, Bangkok, Thailand. His current research interests are design, characterization, and modeling of antennas.

Mitchai Chongcheawchamnan received the BEng degree in telecommunication engineering from King Mongkut's Institute of Technology, Ladkrabang, Thailand in 1992; the MSc degree in communication and signal processing from Imperial College, University of London, UK, in 1995; and the PhD degree in electrical engineering from the University of Surrey, UK. He is currently an associate professor with the Department of Computer Engineering, Faculty of Engineering, Prince of Songkla University, Hat Yai, Songkla, Thailand. From 2007, he serves on the editorial board of *IET Proceedings on Microwaves, Antennas, and Propagation*. His main research areas are high-frequency and microwave applications. He is an IEEE senior member.

Monai Krairiksh received the BEng, MEng, and DEng degrees from King Mongkut's Institute of Technology Ladkrabang (KMITL) in 1981, 1984, and 1994, respectively. In 1981, he joined the KMITL and is presently a professor in the Department of Telecommunication Engineering. He served as the director of the Research Center for Communications and Information Technology (ReCCIT) from 1997 to 2002. Dr. Krairiksh was vice president of the Electrical Engineering/Electronics, Computer, Telecommunications, and Information Technology Association (ECTI) from 2006 to 2007. He is currently an editor of the *ECTI Transactions on Electrical Engineering, Electronics, and Communications*. He was made a senior research scholar of the Thailand Research Fund (TRF) in 2005. His main research interests are antennas for mobile communications and microwave in agricultural applications.